Biomass Conversion and Biorefinery (2024) 14:21507–21521
https://doi.org/10.1007/s13399-024-05474-9

ORIGINAL ARTICLE

Hydrothermal carbonization of sugar beet pulp: optimization and characterization

Zeynep Yıldız Uzun[1]

Received: 15 November 2023 / Revised: 22 February 2024 / Accepted: 27 February 2024 / Published online: 25 May 2024

Abstract
In this study, the optimum hydrothermal conditions of sugar beet pulp were investigated by Response Surface Methodology (RSM) based on Central Composite Design (CCD). The hydrochar obtained from sugar beet pulp (SBP) was optimized for maximum yield and carbon content. Process conditions were chosen with reaction temperatures of 200–240 °C, residence time 60–150 min, and biomass to water ratio of 1:3–1:10. The yield and carbon content of the hydrochar varied with the process parameters. In order to obtain hydrochar with the highest yield and carbon content in optimization, the reaction temperature should be 220.74 °C, the biomass to water ratio should be 1:3, and the residence time should be 95.58 min. High heating value, energy and mass yield, and energy densification ratio of sugar beet pulp and hydrochar were also investigated. The products were characterized using FT-IR, SEM, and ultimate analysis techniques. The Coats-Redfern method was used to estimate the kinetic parameters of the combustion processes. The activation energy values of SBP and SBP-HC products were calculated as 13.88 and 11.46 kJ/mol, respectively. The kinetic data were used to determine the thermodynamic parameters (ΔH, ΔG, and ΔS). As a result, the properties of hydrochar produced from sugar beet pulp under optimum conditions have been extensively investigated and the results have shown that hydrochar has potential for use in different areas.

Keywords Biomass · Hydrothermal carbonization · Central Composite Design · Response Surface Methodology · Sugar beet pulp

1 Introductıon

Food waste is generated throughout the supply chain, beginning from agricultural generation to mass production, distribution, and eventually, household consumption. Food waste is primarily derived from household kitchens, food processing sites, and canteens, and it is considered among the greatest organic solid waste groups that are produced globally, with the generation rate continually growing [1]. Hydrothermal carbonization (HTC) has the added advantage of being useful in the treatment of a wider range of feedstocks, including food waste that contains high levels of moisture. Throughout the HTC process, intricate chemical reactions are applied to organic matter containing lignocellulosic, resulting in the creation of solid hydrochar and liquid substances that are rich in carbon [2]. In addition, HTC is one of the thermochemical conversion technologies. It is also a technological process that transforms biomass into value-added materials [3]. In the HTC process, the raw material is heated in the medium temperature range (180–300 °C). In the hydrothermal carbonization method, the pressure is self-generated. The solid product formed at the end of hydrothermal carbonization is called hydrochar [4]. Hydrochar produced as a result of hydrothermal carbonization is formed as a result of many consecutive reactions (decarboxylation, decarbonylation, dehydration) [5]. The HTC process must be tightly controlled below the subcritical water range. Compared to normal water, subcritical water contains a high concentration of H^+ ions, which is a natural medium that promotes acid-catalyzed reactions of organic compounds [6]. With the hydrothermal carbonization method, excessive energy use is prevented and biomass energy is recovered in the presence of water, because hydrothermal carbonization contributes to the natural carbonization process produced from biomass within a few hours [7]. In the literature, many scientists have investigated the formation of hydrochar

✉ Zeynep Yıldız Uzun
zyildiz@sinop.edu.tr

[1] Boyabat Vocational School, Department of Chemistry and Chemical Processing Technologies, Sinop University, Sinop, Turkey

(biofuel) using different biomass by hydrothermal carbonization method. For example, Yu et al. [8], it was reported that the heating values of hydrochar products obtained by hydrothermal carbonization of waste ginkgo leaf residues at different temperatures (100–220 °C) vary in the range of 19.1–22.1 MJ/kg. Another example is a study by Nawaz and Kumar [5]. They produced hydrochar from sunflower stalks by hydrothermal carbonization method at different temperatures (180, 230, and 280 °C). While the high heating value of raw sunflower stalks was 19.81 MJ/kg, the highest calorific value was reported as 26.85 MJ/kg among hydrochar products. Hydrothermal carbonization (HTC) technology is a suitable method for food waste treatment. Because from an economic perspective, the pre-drying step that causes additional costs can be eliminated in the HTC process [1]. In addition, there are studies in the literature on hydrothermal carbonization of food waste. For example, hydrochar products were obtained from food waste by hydrothermal carbonization method at 200, 230, and 260 °C for 30 min. It was reported that the HHV value of food waste was increased from 25.1 to 33.1 MJ kg^{-1} by HTC [9].

Response Surface Methodology (RSM) is one of the most used multi-techniques for the optimization of processes. Experimental design allows examining process conditions to obtain materials with adequate responses with statistical accuracy [10]. RSM is a powerful technique used to test different process parameters by performing a minimum number of experimental traces. In general, RSM is defined as a collection of mathematical and statistical tools [11]. Biomass also includes biodegradable wastes from the agriculture and food industries, such as the sugar industry [12]. Sugar beet pulp is a by-product of the sugar industry and waste pulp can often be used as cattle feed [13]. For example, Wilk et al. [12], hydrochar products were obtained from beet pulp waste by hydrothermal carbonization at different temperatures (180, 200, and 220 °C) and at different times (1, 2, 3, and 4 h). It has been reported that the high heating values of hydrochar products vary in the range of 19.61–25.36 MJ/kg [12]. In another literature study, it was reported that porous carbon was produced from sugar beet pulp biomass by hydrothermal carbonization [13].

In this study, the effects of temperature, biomass to water ratio and residence time on hydrochar obtained from sugar beet pulp by hydrothermal carbonization method were investigated. Optimum conditions were determined for the hydrothermal carbonization of sugar beet pulp. In order to determine the optimum conditions, the Design Expert software program and the Response Surface Method based on the Center Composite Design (CCD) were applied. The hydrochar produced under optimum conditions was characterized using techniques such as FT-IR, SEM, and elemental analysis. In addition, fuel properties (mass yield, energy yield, and HHV) and combustion behavior of the products were also investigated. The results showed that the fuel properties of the hydrochar product obtained from sugar beet pulp under optimum conditions were improved by HTC. In addition, this study is an original study in which biofuel production is investigated by considering different process parameters (Tables 1, 2, 3 and 4).

2 Materials and methods

2.1 Preparation of raw materials

Sugar beet pulp (SBP) was collected from a sugar factory in Turkey. For characterization of raw SBP, it was dried in an oven at 80 °C for 10 h. SBP was ground and then sieved. SBP was characterized using different analysis techniques (FT-IR, SEM, and Ash and Ultimate analysis).

2.2 Hydrothermal carbonization experiment

A pressure reactor with a volume of 40 mL was used to conduct the HTC experiments. The amount of deionized water specified in the process conditions was added to a 1-g sample. Then, 20 experiments were carried out at different temperatures and times (Table 5). After the experiment was finished, the reactor was cooled to room temperature. After the experiment, the solid products were weighed and the yield was calculated. In addition, the %carbon content of solid products (hydrochars) was determined by elemental analysis results. The hydrochar produced in optimum condition by HTC was symbolized as SBP-HC.

2.3 Characterization of products

Ash analysis, elemental analysis, high heating value, energy and mass yields, and energy densification ratio of SBP and SBP-HC products were determined. HHV, energy densification, energy yield, and fuel ratio of product were calculated using the following Eqs. (1–4) [14–16].

$$\mathrm{HHV} = (0.338 \times C) + 1.428 \times \left(H - \frac{O}{8}\right) + (0.095 \times S) \quad (1)$$

Table 1 Experimental ranges and levels of independent variables

	Experimental levels				
Independent variables	−α	−1	0	1	+α
Reaction temperature (°C)	200	208	220	231	240
Residence time (min)	60	78	105	131	150
Biomass to water ratio	1:3	1:4.4	1:6.5	1:8.5	1:10

Table 2 Ash and ultimate analysis of products

Materials	Ash analysis (%)	Ultimate analysis (%)					HHV (MJ/kg)
		C	***H***	***N***	***S***	***O***	
SBP	6.7	40.53	6.39	1.49	0.19	51.4	13.67
SBP-HC	5.6	47.50	5.59	1.76	0.06	45.09	16.00

Table 3 Combustion parameters of SBP and SBP-HC

Sample	T_i (°C)	T_b (°C)	T_m (°C)	$-\Delta TG_{max}$ (%/min)	$-\Delta TG_{mean}$ (%/min)	$S \times 10^{-6}$ ($\%^2/°C^3.min^2$)
SBP	227	513	413	73.93	2.48	6.94
SBP-HC	262	493	449	96.72	2.40	6.86

Table 4 Combustion kinetic and thermodynamic parameters of SBP and SBP-HC

Sample	Linear function	E_a (kJ/mol)	A (min^{-1})	R^2	ΔH, kJ/mol	ΔG, kJ/mol	ΔS, kJ/mol.K
SBP	$y = -1669.4 \times -6.3209$	13.88	879.66	0.9815	8.18	165.96	−0.229
SBP-HC	$y = -1378.6 \times -7.7777$	11.46	169.35	0.9061	5.46	181.63	−0.244

Table 5 Experimental design matrix and the corresponding response results

Experiment number	Reaction temperature (°C)	Residence time (min)	Biomass to water ratio	Hydrochar yield (%)	Hydrochar carbon content (%)
1	208	131	1:8.5	67.14	44.62
2	220	105	1:6.5	72.86	43.70
3	220	105	1:6.5	71.43	45.76
4	240	105	1:6.5	61.43	46.57
5	220	105	1:10	74.29	47.15
6	208	78	1:8.5	72.86	44.57
7	200	105	1:6.5	70.42	40.74
8	231	78	1:4.4	70.35	47.59
9	208	131	1:4.4	68.57	46.93
10	220	105	1:6.5	69.44	46.70
11	220	60	1:6.5	73.61	43.53
12	220	150	1:6.5	64.79	48.90
13	220	105	1:6.5	66.20	48.57
14	220	105	1:6.5	67.61	48.37
15	231	131	1:8.5	62.86	50.08
16	220	105	1:3	68.49	47.96
17	220	105	1:6.5	70.42	49.67
18	208	78	1:4.4	76.06	44.88
19	231	131	1:4.4	65.71	52.29
20	231	78	1:8.5	62.86	48.38

$$\text{Energy densification ratio} = \frac{\text{HHV of hydrochar}}{\text{HHV ofsugar beet pulp}} \quad (2)$$

$$\text{Hydrochar yield}(\%) = \frac{M_{\text{Hydrochar}}}{M_{\text{biomass}}} \times 100 \quad (3)$$

$$\text{Energy yield}\ (\%) = \text{mass yield} \times \text{energy densification} \quad (4)$$

FT-IR spectrum of SBP and SBP-HC products were recorded using the Fourier Transform Infrared Spectrometer. The spectrum wave number was between 650 and 4000 cm^{-1}. The *%C*, *H*, *N*, and *S* values of the products were determined using an elemental analyzer. SEM analysis was performed to determine the surface properties and three-dimensional images of the products were taken. The sizing of SEM images of SBP and SBP-HC was taken as 10 µm.

2.4 Thermogravimetric analysis of products

Thermal behavior of SBP and SBP-HC was performed on the thermogravimetric analyzer (SDTQ600). Ten milligrams of sample was added to the holder in the device. The temperature was increased to 800 °C and the heating rate was chosen as 20 °C/min. During combustion, the airflow rate was 30 mL/min. The mass loss rates of the samples depending on the temperature were recorded on the computer as a function of temperature and time.

2.5 Combustion analysis of products

The TG and DTG curves of the products (SBP and SBP-HC) were used to determine the combustion parameters. Combustion parameters were determined as ignition temperature (T_i), combustion temperature (T_b), and maximum peak temperature (T_m), respectively. The *S* value (comprehensive combustibility index) of the raw material and hydrochar product was calculated using Eq. 5 below [15].

$$S = \frac{(\frac{d_W}{d_t})_{max} \times (\frac{d_W}{d_t})_{mean}}{T_i^2 \times T_b} \quad (5)$$

2.6 Kinetic analysis

Kinetic parameters (activation energy and pre-exponential factor) of the degradation reactions of SBP and SBP-HC products were calculated using the Coats-Redfern Model given in the literature. The change in mass and temperature during the combustion process is defined as follows:

$$\frac{d\alpha}{dT} = \frac{A}{\beta} e^{\frac{-E_a}{RT}(1-\alpha)^n} \quad (6)$$

where *A* stands for pre-exponential factor, *E* represents the activation energy, and *n* stands for reactor order. The Eq. (7) used in the Coats-Redfern method and simplified by accepting the first-order reaction rate expression is given below [17, 18].

$$\ln\left[\frac{-\ln(1-\alpha)}{T^2}\right] = \ln\frac{AR}{\beta E_a} - \frac{E_a}{RT}(n=1) \quad (7)$$

The graph of $\ln\left[\frac{-\ln(1-\alpha)}{T^2}\right]$ against 1/T was plotted to determine activation energy. The activation energy (E_a) is calculated from the slope of lines.

2.7 Determination of thermodynamic parameters

Kinetik parametreler kullanılarak (E_a ve A) termodinamik parametreler (enthalpy, Gibbs free energy, and entropy) hesaplanabilir. These parameters can be calculated using the following equations [19].

$$\text{Enthalpy}(\Delta H) = E_a - RT \quad (8)$$

$$Entropy(\Delta S) = R \times \ln(\frac{Ah}{KT}) \quad (9)$$

$$Gibbsfreeenergy(\Delta G) = \Delta H - T\Delta S \quad (10)$$

where *h* is Planck's constant and *K* is the Boltzmann constant.

2.8 Design of experiments

Many experiments and literature research are required to determine the optimum conditions for the hydrochar product using process variables. For this reason, Design Expert software proposed a set of 20 experiments using three process parameters (reaction temperature, residence time, and biomass to water ratio) and two responses (hydrochar yield, hydrochar carbon content). Design Expert software program was used to reduce the number of experiments and to examine the effect of process parameters on the product. Twenty experiments suggested by the software were performed. Table 5 shows the response results obtained as a result of the experiments. The Response Surface Method, a mathematical technique, was used to design experiments and optimum conditions were determined. Optimal reactions were studied at temperatures between 200 and 240 °C, over a period of 60 to 150 min, with a biomass to water ratio of 1:3 to 1:10.

ANOVA test was performed to evaluate the reliability of the selected model. In this study, Central Composite Design was used with Surface Response Method for hydrthermal carbonization experiments. It is possible to obtain optimum working conditions by considering the response values.

High %carbon content and high %yield amounts of hydrochar products are defined as experimental response. The independent variables are coded in the range of $-\alpha$ and $+\alpha$ values. The variables and experimental range in this design are presented in Table 1. Twenty experiments consisting of 8 cube (facto-rial) points, 6 centers, and 6 axial points were generated according to Eq. (11) [20].

$$N = 2^n + 2n + n_c = 2^3 + 2 \times 3 + 6 = 20 \tag{11}$$

where N is the number of experiments, n is the number of factors, and n_c is the number of replicates at the center point. Regression analysis of the experimental data was determined using a quadratic polynomial expression specified in Eq. (12).

$$Y = \beta_0 + \sum_{i=1}^{n} \beta_1 X_i + \sum_{i=1}^{n} \beta_{ii} X_i^2 + \sum_{i=1}^{n} \sum_{j>1}^{n} \beta_{ij} X_i X_j + \varepsilon \tag{12}$$

Y is defined as the response variable (%hydrochar yield and %hydrochar carbon content). X_i and X_j are independent control variables. n is the number of experiments, and β_o, β_i, β_{ii}, and β_{ij} are regression coefficients for the constant, linear, quadratic, and interaction terms, respectively. ε is statistical error [21].

2.9 Statistical analysis

Regression analysis was performed using the ANOVA test to show the compatibility of the experimental data with the method in Central Composite Design (CCD) and the experimental results. Additionally, the coefficient of determination R^2, adjusted R^2, predicted R^2, lack of fit, adequate precision, F value, and P value were used to determine the selection, precision, and reliability of the best model. The model with a P value less than 0.05 was considered significant.

3 Results and discussion

3.1 Ash and ultimate analysis

Ash and elemental analysis (%C, H, N, and S) of SBP and SBP-HC products were performed. The results obtained are presented in Table 2. The ash values of SBP and SBP-HC products were calculated as 6.7 and 5.6, respectively. Biomass ash contents generally vary between 0.1 and 25% [22]. It can be said that the ash content of raw SBP is low when compared to the ash content of raw biomass in the literature. In addition, ultimate analysis results of hydrochar products have also been reported in the literature. According to the results of elemental analysis, the %carbon content (%C) values of hydrochar products vary between 23.94 and 87.08%, respectively [23]. It can be said that the carbon content of the SBP-HC product produced under optimum conditions in this study is within the range reported in the literature. The higher the carbon contents of hydrochar products, the higher the quality [23]. Biomass has a low energy density; therefore, it is a low-quality fuel [24]. Hydrochar, which is obtained from biomass by hydrothermal carbonization method, is a coal-like material and contains a large amount of carbon. Increasing the carbon value provides an increase in the high heating value of hydrochar products [15, 25]. An important indicator describing the energy potential of a fuel is its high heating value [12]. The carbon content of SBP and SBP-HC was measured as 40.53 and 47.50, respectively. As seen in Table 2, the carbon content of the SBP-HC product is higher than the SBP product. Literature studies were examined in terms of high heating values of hydrochar products. For example in a study reported in the literature, the carbon content of beet pulp hydrochar obtained after 1 and 2 h at 220 °C was 55.1–56.8%, respectively. In addition, high heating value of the hydrochar obtained after 1 and 2 h at 220 °C was found to be 22.10–23.35 MJ/kg, respectively [12]. For example, in a study by Cheng et al. [14], hydrochar was obtained as a result of hydrothermal carbonization of coconut waste shell waste at 220 °C and 1-h reaction time, and its maximum high heating value was reported as 29.39 MJ/kg. In another literature study, the highest high heating value of the hydrochar product obtained as a result of hydrothermal carbonization from corn stalk biomass was reported as 22.82 MJ/kg [26].

The HHV value of the SBP-HC product obtained in this study is higher than the raw product. This result shows that the SBP-HC product has better biofuel properties compared to the SBP product when evaluated in terms of HHV. At the same time, the fuel properties of hydrochar products can be interpreted by taking into account parameters such as energy densification ratio and energy yield (%). The energy densification ratio of the SBP-HC product was calculated as 1.17. For example, as a result of the hydrochar product obtained from rice husk biomass, the maximum energy densification ratio was reported as 1.39 [17]. The energy efficiency of hydrochars is directly proportional to their mass yield [18]. In this study, the energy yield (%) of the hydrochar product produced under optimum conditions was calculated as 83.34.

3.2 FT-IR analysis

FT-IR analysis was used to investigate the effect of HTC conditions on the structural properties of SBP and SBP-HC products. FT-IR spectra of SBP and SBP-HC products are presented in Fig. 1. When the spectra of the products are examined, the peak seen at approximately 3300 cm^{-1} is the O–H stretching vibration. This peak appears wider

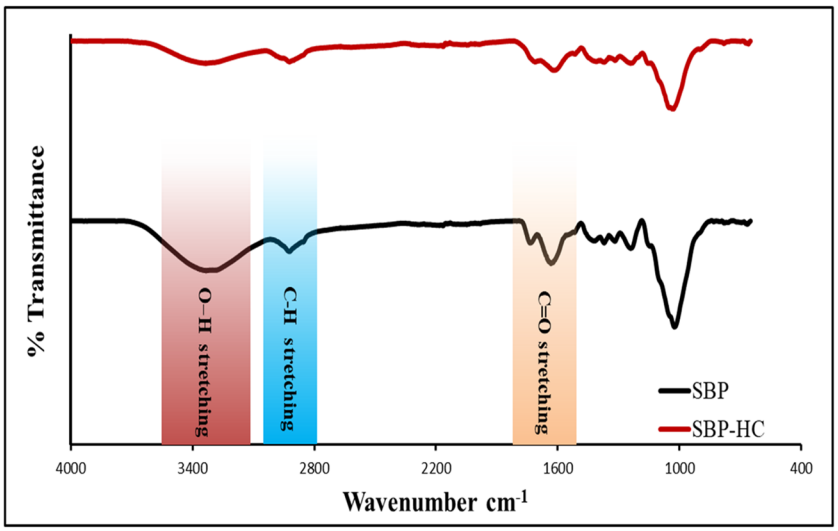

Fig. 1 FTIR analysis of biomass and hydrochar

in the FTIR spectrum of SBP. In addition, these peaks can be caused by phenol, alcohol, water, and acid. The vibration peak of –OH in hydrochar decreases significantly with increasing HTC temperature [27]. The peaks observed in the range of 2800–2950 cm^{-1} are the C-H stretching vibrations of the aliphatic methyl and methylene groups [5].

C=O stretching vibrations of SBP and SBP-HC in the spectrum are seen at 1654 and 1655 cm^{-1}, respectively. These peaks may belong to carbonyl and ester-derived compounds in the structure. This vibration peak decreases significantly during the hydrothermal process due to dehydration and decarboxylation reactions. [28]. It can be said that the peaks in the range of 1000–1200 cm^{-1} belong to C-O and C–O–C stretching vibrations. Similar results are consistent with the FT-IR spectra of sugar beet pulp and hydrochar products reported in the literature [12, 29]. Hydrochar products can show high adsorption capacity due to the rich functional groups on their surface [30].

3.3 SEM analysis

SEM analysis was performed to examine the surface morphology of SBP and SBP-HC products. SEM analysis gave information about the general surface structures of the products. SEM images of the products are shown as 10 µm and presented in Fig. 2. When the SEM images are examined, the structural properties of the samples change with HTC.

In addition to having a fibrous structure, we can say that the raw biomass (SBP) has almost no pores in the structure. When the SEM images of the SBP-HC product are examined, it is seen that it has a slightly porous structure as well as exhibiting a fibrous structure. With HTC, we can say that a small amount of porosity is formed in the hydrochar product compared to the raw biomass. Since hydrochar has a porous structure, it can be preferred as an adsorbent in adsorption studies. As the porosity increases, the adsorption performance of adsorbents can increase. Especially in recent years, it has been reported that hydrochar products produced from different biomass wastes have a porous structure and are used in adsorption studies [10, 31]. Hydrochar products have been reported to be used as adsorbents in the removal of heavy metals [32], methylene blue [33], and antibiotics [34].

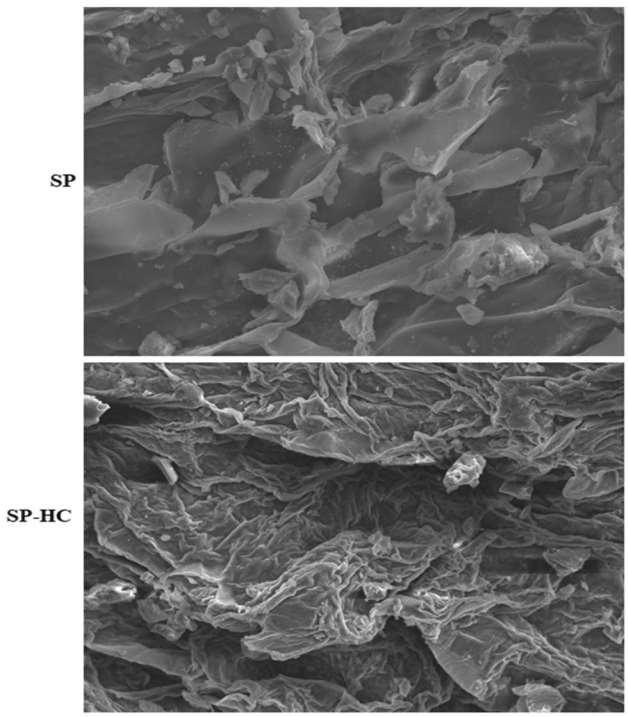

Fig. 2 SEM images of SBP and SBP-HC

3.4 Thermogravimetric analysis

Thermogravimetric analysis of SBP and SBP-HC was carried out by heating from room temperature to 800 °C in an air atmosphere at a heating rate of 20 °C/min. The thermogravimetric curves (TG and DTG) of the thermal decomposition of the products are presented in Fig. 3. When DTG curves are examined; the decomposition of both products (SBP and SBP-HC) took place in two steps. In the first step of the SBP product, a mass loss was observed in the temperature range of 228–379 °C. When the DTG curves are examined, the second step in SBP is in the temperature range of 380–512 °C. Hemicellulose, cellulose, and lignin have been reported to decompose at temperatures ranging from 215–315 °C, 315–450 °C, and 200–900 °C, respectively [5]. In the first step of the SBP-HC, it was observed as mass loss in the temperature range of 257–392 °C. The second (main) decomposition in SBP-HC is in the temperature range of 392–498 °C and the weight loss is 80.05%.

3.5 Combustion analysis

Combustion parameters (T_i, T_b, and T_m) of SBP and SBP-HC products were estimated using thermogravimetric (TG) and differential thermogravimetric (DTG) curves. T_i (ignition temperature) values show the thermal stability of different biomass samples. As the T_i values of hydrochar products increase, their thermal stability increases [5]. In addition, the ignition temperature (T_i) is taken into account when it comes to the storage and safety of fuels. If the T_i value is high, the spontaneous combustion of hydrochar products is reduced, and therefore, hydrochar becomes a safe fuel [35].

Combustion parameters of SBP and SBP-HC are presented in Table 3. T_i values of SBP and SBP-HC products are 227 and 262 °C, respectively. As can be seen, the T_i value of the SBP-HC product is higher than the raw biomass. For example, similar to our study, it has been reported that the T_i value of hydrochar products produced from waste ginkgo leaf residues is higher than that of crude biomass [8]. In addition, it has been reported in the literature that the hydrochar product obtained from sugar beet at 220 °C has a higher T_i value [12]. T_b (burnout temperature) values of SBP and SBP-HC products were determined as 513 and 493 °C, respectively. This result showed that the combustion process of SBP was longer than that of the hydrochar product. It can be said that the S index values of SBP and SBP-HC products are similar (Table 3).

3.6 Kinetic and thermodynamic analysis

TG and DTG graphs drawn using mass loss data were used to examine the combustion kinetics of SBP and SBP-HC products. Determination of kinetic parameters is very important for the efficiency of a facility to be established and operated [36]. Kinetic parameters are crucial for the accurate prediction of thermal decomposition of solid fuel [37].

Linear line graphs were drawn using thermogravimetric analysis results and the Coats-Redfern equation. Using the pilot curves shown in Fig. 4, activation energy (E_a, kJ/mol) and pre-exponential factor (A, min^{-1}) values of SBP and SBP-HC products were calculated. In addition, the results of kinetic parameters are shown in Table 4. The correlation coefficients (R^2) of crude SBP and SBP-HC products are greater than 0.90. In addition, the activation energy values

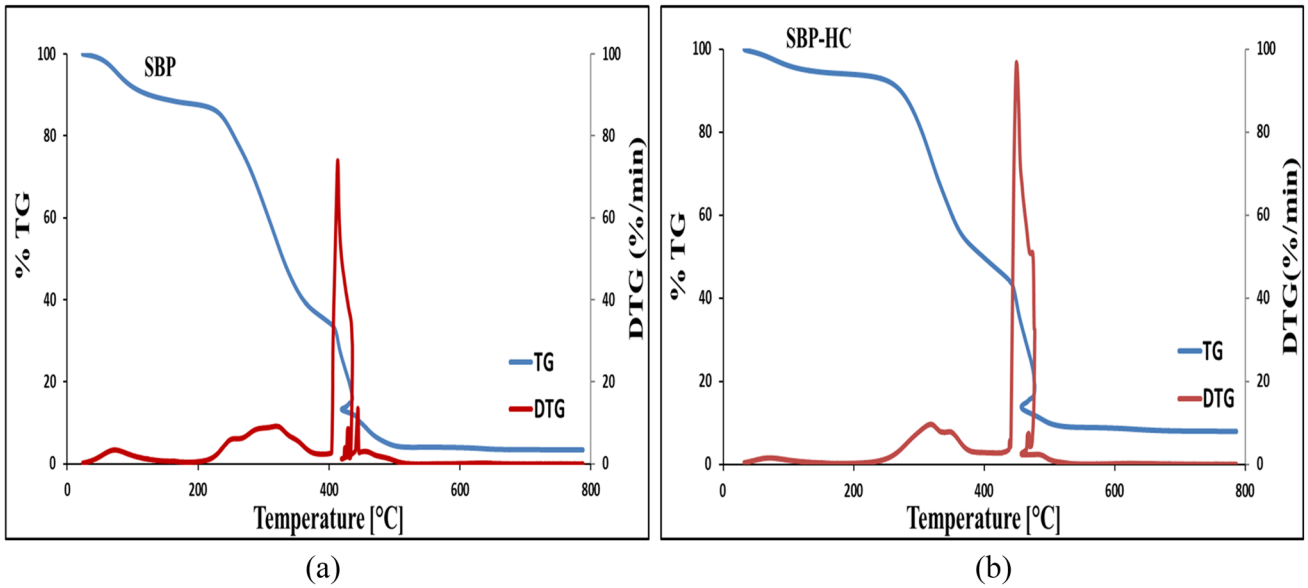

Fig. 3 TG and DTG curves of SBP (**a**) and SBP-HC (**b**)

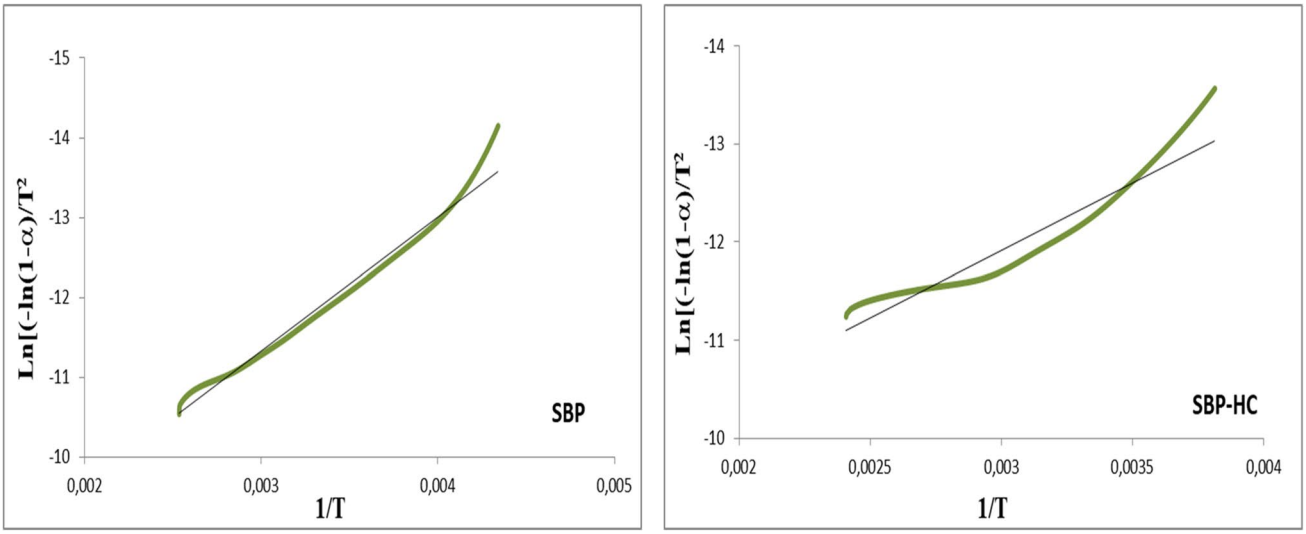

Fig. 4 Plot curves for SBP and SBP-HC

(E_a) of SBP and SBP-HC products were calculated as 13.88 and 11.46 kJ/mol, respectively. A decrease in the activation energy value of the hydrochar product produced under optimum conditions is observed compared to the raw material.

Many researchers have used the Coats-Redfern method to estimate the kinetic parameters for the combustion processes of different biomass and hydrochars [27, 38]. There are few studies in the literature on the combustion kinetics of SBP. In this study, using thermogravimetric analysis data, activation energy values of the raw material and the hydrochar product produced under optimum conditions were calculated and it was seen that these values are lower than other hydrochars reported in the literature [12].

Thermodynamic parameters (ΔH, ΔG, and ΔS) for SBP and SBP-HC products were calculated using Eqs. 8–10 and these values are presented in Table 4. The heat content of a system is called enthalpy. Enthalpy change (ΔH) at constant pressure is the amount of energy released by any process. In exothermic processes, ΔH is negative. Positive ΔH values represent endothermic reactions that require energy from the environment [39]. When Table 4 is examined, the ΔH values calculated in this study are positive. Positive ΔH values indicate that energy is needed to initiate the combustion reactions of SBP and SBP-HC products. In this study, ΔH values calculated for SBP and SBP-HC are 8.18 and 5.46 kJ/mol, respectively. Increasing ΔH value indicates increasing energy need. For example, the ΔH value for Albizia lebbeck seed pods was reported to be 151.16 kJ/mol [19]. Positive ΔH values indicate that energy is required to start the reaction [39]. The increase in ΔG values also indicates that the reaction is gradually becoming non-spontaneous and becoming more difficult to occur [19]. The ΔG values of SBP and SBP-HC products are positive and represent the non-spontaneous process. The ΔG value of the SBP-HC product is higher than the SBP product. The parameter ΔS is a measure of disorder in a system. A high ΔS value represents that the system is far from its thermodynamic equilibrium [40]. When Table 4 is examined, irregularity increased as the SBP-HC product was obtained under optimum conditions.

3.7 Design of experiments

The effects of process parameters (reaction temperature, residence time, and biomass to water ratio) on hydrochar yield and carbon content were determined using the Response Surface Method. RSM is a mathematical and statistical technique used to build empirical models to optimize the response affected by the independent variable [41]. The Design-Expert software proposes a series of experiments (20 experiments) based on the combination of these three process parameters. Reaction temperature (°C), residence time (min), and biomass to water ratio were chosen as 200–240 °C, 60–150 min, and 1:3–1:10, respectively. Table 5 shows the number of experiments based on the combination of these three parameters. (%) Hydrochar yield and (%) hydrochar carbon content are the response values in the design. Optimal process parameters were determined using ANOVA.

3.8 Statistical analysis

Analysis of variance (ANOVA) was performed by considering the quadratic model in the Central Composite Design technique. ANOVA was used to examine the effects of independent process parameters (reaction temperature,

biomass to water ratio, and residence time) on responses (hydrochar yield and hydrochar carbon content). A model is significant with a larger *F*-value and lower *P* value. The *P* value, used to validate the hypothesis against experimental data, is the most widely used statistical calculation [21]. If the *P* value is less than 0.05, the independent variables in the model are significant [41]. A high *F* value indicates reliability and reproducibility [42]. Table 6 shows the ANOVA analysis results. *F* value for %hydrochar yield is 3.54 (Table 6). This value shows that the model is important. The "lack of fit" value is 0.3337 and this value is not significant. In order to obtain a reliable and accurate regression model, the "lack of fit" value should be not significant [11]. The same is true for the %carbon content of

Table 6 Analysis of variance ANOVA for %hydrochar yield

Source	Sum of squares	df	Mean square	*F* value	*P* value	Status
Model	240	9	26.67	3.54	0.0309	Significant
A, reaction temperature	105.56	1	105.56	14.00	0.0038	
B, residence time	78.22	1	78.22	10.37	0.0092	
C, biomass to water ratio	1.99	1	1.99	0.26	0.6185	
AB	9.18	1	9.18	1.22	0.2957	
AC	4.08	1	4.08	0.54	0.4792	
BC	5.14	1	5.14	0.68	0.4285	
A^2	29.20	1	29.20	3.87	0.0775	
B^2	1.02	1	1.02	0.13	0.7213	
C^2	3.73	1	3.73	0.49	0.4979	
Residual	75.42	10	7.54			
Lack of fit	45.25	5	9.05	1.50	0.3337	Not significant
Pure error	30.17	5	6.03			
Cor total	315.42	19				
Std. Dev		2.75			*R*-squared	0.7609
Mean		68.87			Adj *R*-squared	0.5457
C.V		3.99			Pred *R*-squared	0.2324
PRESS		388.73			Adeq precision	7.331

Table 7 Analysis of variance ANOVA for %carbon content

Source	Sum of squares	df	Mean square	*F* value	*P* value	Status
Model	100.36	9	11.15	3.19	0.0424	Significant
A, reaction temperature	53.95	1	53.95	15.45	0.0028	
B, residence Time	22.50	1	22.50	6.44	0.0294	
C, biomass to water ratio	2.14	1	2.14	0.61	0.4522	
AB	2.31	1	2.31	0.66	0.4349	
AC	0.18	1	0.18	0.052	0.8250	
BC	3.12	1	3.12	0.89	0.3665	
A^2	10.95	1	10.95	3.13	0.1071	
B^2	0.016	1	0.016	0.00464	0.9470	
C^2	3.71	1	3.71	1.06	0.3271	
Residual	34.93	10	3.49			
Lack of fit	11.04	5	2.21	0.46	0.7916	Not significant
Pure error	23.89	5	4.78			
Cor total	135.29	19				
Std. Dev		1.87			*R*-squared	0.7418
Mean		46.85			Adj *R*-squared	0.5094
C.V		3.99			Pred *R*-squared	0.1279
PRESS		117.98			Adeq precision	7.685

hydrochar. The model F value is 3.19 and the corresponding lack of fit is 0.7916 (Table 7). "Prob > F" values less than 0.0500 indicate that the model terms are meaningful. In addition, values greater than 0.1000 indicate that the model is not significant [43]. As a result, the ANOVA results for hydrochar yield and hydrochar carbon content obtained by hydrothermal carbonization of sugar beet pulp show a high F value, which indicates that the developed regression model is significant. In this study, the coefficient of determination, R^2 for the %hydrochar yield and hydrochar %carbon content model is 0.7609 and 0.7418, respectively. The R^2 value shows a good accordance in the design between the results obtained and calculated. The coefficient of variation (%C.V.) is the error expressed as a percentage of the mean. A low %C.V. (~ 10%) is considered a good indicator for the reproducibility of the model [11]. In this study, the value of %C.V. for both %hydrochar yield and hydrochar %carbon content is 3.99 and this value is relatively low. Another regression parameter to be noted is adjusted R^2. Adjusted R^2 refers to the amount of variation that can be explained by the model [11]. In this study, the adjusted R^2 for the %hydrochar yield and hydrochar %carbon content model is 0.5457 and 0.5094, respectively. "Adequate precision" measures the signal to noise ratio. This value is required to be greater than 4. [11]. "Adequate precision" for %hydrochar yield and hydrochar %carbon content are 7.331 and 7.685. These values also show the suitability of the model.

Figure 5 shows the effect of process parameters (reaction temperature, biomass to water ratio, and residence time) on the yield and carbon content of hydrochar. The reaction temperature, biomass to water ratio, and residence time were kept at a fixed point of 220 °C, 6.5, and 105 min, respectively. The effect of reaction temperature, biomass to water ratio, and residence time on the yield and carbon content of hydrochar was investigated and 3D graphics are presented in Fig. 5. According to the graphics, when the residence time is kept constant in the center (105 min), the yield decreases with increasing temperature, but the carbon content increases. When the temperature is kept constant in the center (220 °C), the yield decreases with the increase in residence time, but the carbon content increases. With the increase in reaction temperature and residence time, an increase in the amount of carbon is observed. When the reaction temperature and residence time were kept constant (220 °C and 105 min), the yield decreased with the increase in the biomass water ratio. As a result, it was seen that reaction temperature, residence time, and biomass to water ratio affect on the yield and carbon amount of hydrochar. It has been reported in the literature that hydrochar products with higher HHV are obtained by increasing the reaction temperature and residence time [44, 45].

3.9 Optimization

In order to produce hydrochar under optimum conditions with the hydrothermal carbonization method of SBP, Surface Response Method and Central Composite Design were used. The design was carried out using parameters at certain intervals. Reaction temperature, biomass to water ratio, and residence time and responses (yield and carbon content of hydrochar) are given in Table 5. The reaction temperature, biomass to water ratio, and residence time were chosen as 200–240 °C, 1:3–1:10, and 60–150 min, respectively. The yield of hydrochar varies between 61.43 and 76.06% under different process conditions. The carbon content of hydrochar varies between 40.74 and 52.29%. Analysis of variance (ANOVA) for %hydrochar yield and hydrochar %carbon content is given in Table 6 and 7. The relationship between the responses (%hydrochar yield and hydrochar %carbon content) and the independent variables can be expressed by the following polynomial equation.

$$\%\text{hydrochar yield} = 69.68 - 2.78 \times A - 2.39 \times B - 0.38 \times C + 1.07 \times A \times B - 0.71 \times A \times C + 0.8 \times B \times C - 1.42 \times A^2 - 0.27 \times B^2 + 0.51 \times C^2$$

$$\%\text{carbon content of hydrochar} = 47.07 + 1.99 \times A + 1.28 \times B - 0.40 \times C + 0.54 \times A \times B + 0.15 \times A \times C - 0.62 \times B \times C - 0.87 \times A^2 + 0,034 \times B^2 + 0.51 \times C^2$$

A, B, and C represent reaction temperature (°C), biomass to water ratio, and reaction time (min), respectively. In order to investigate performance of hydrochar, the yield and carbon content of the hydrochar were selected as maximum. In the optimization process, reaction temperature (°C), residence time (min), and biomass to water ratio were determined as 220 °C, 96 min, and 1:3, respectively, to produce hydrochar with high yield and high carbon content. For example, in a study by Kang et al. [26], the optimization of hydrothermal carbonization for corn stalk was performed using process parameters such as reaction temperature, residence time, and biomass loading.

In another study, it was reported that hydrochar was produced in different process parameters (temperature, time, and water: precursor ratio) by hydrothermal carbonization method from coffee husk. For optimization, a central composite rotatable design method based on Response Surface Methodology was used [10]. After the optimum experimental conditions were determined, the validation test was performed. The experimental results and the results obtained by the model were compared and presented in Table 8. Modeled results (72.91) and experimental results (71.23) showed consistent good agreement with each other for maximum hydrochar yield. There is a similar situation for the %carbon content of the hydrochar product. The modeled and experimental results for the maximum amount of carbon are 48.45 and 47.50, respectively.

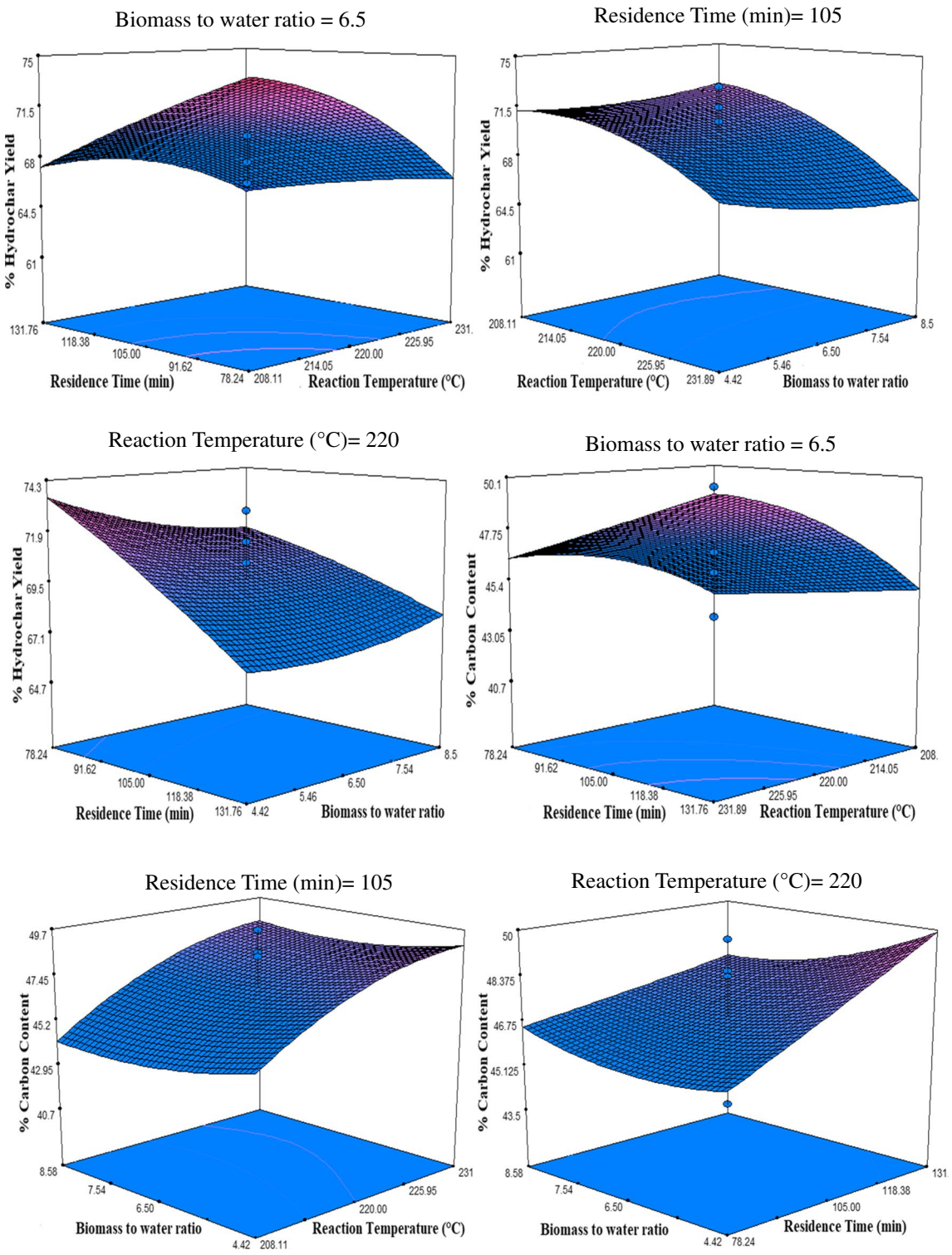

Fig. 5 Effect of reaction temperature, residence time, and biomass to water ratio

3.10 Mechanism of hydrothermal carbonization

In general, the hydrothermal carbonization reaction mechanism consists of hydrolysis, dehydration, decarboxylation, condensation polymerization, and aromatization stages. Food waste normally has complex chemical compositions of lipids, proteins, and carbohydrates [46]. These three components are observed to significantly influence the structure of

Table 8 Model validation

Optimized process parameters			Response	
Reaction temperature (°C)	Residence time (min)	Biomass to water ratio	Hydrochar yield (%)	Hydrochar carbon amount (%)
220.74	95.58	1:3	Predicted, 72.91 Experimental, 71.23	Predicted, 48.45 Experimental, 47.50

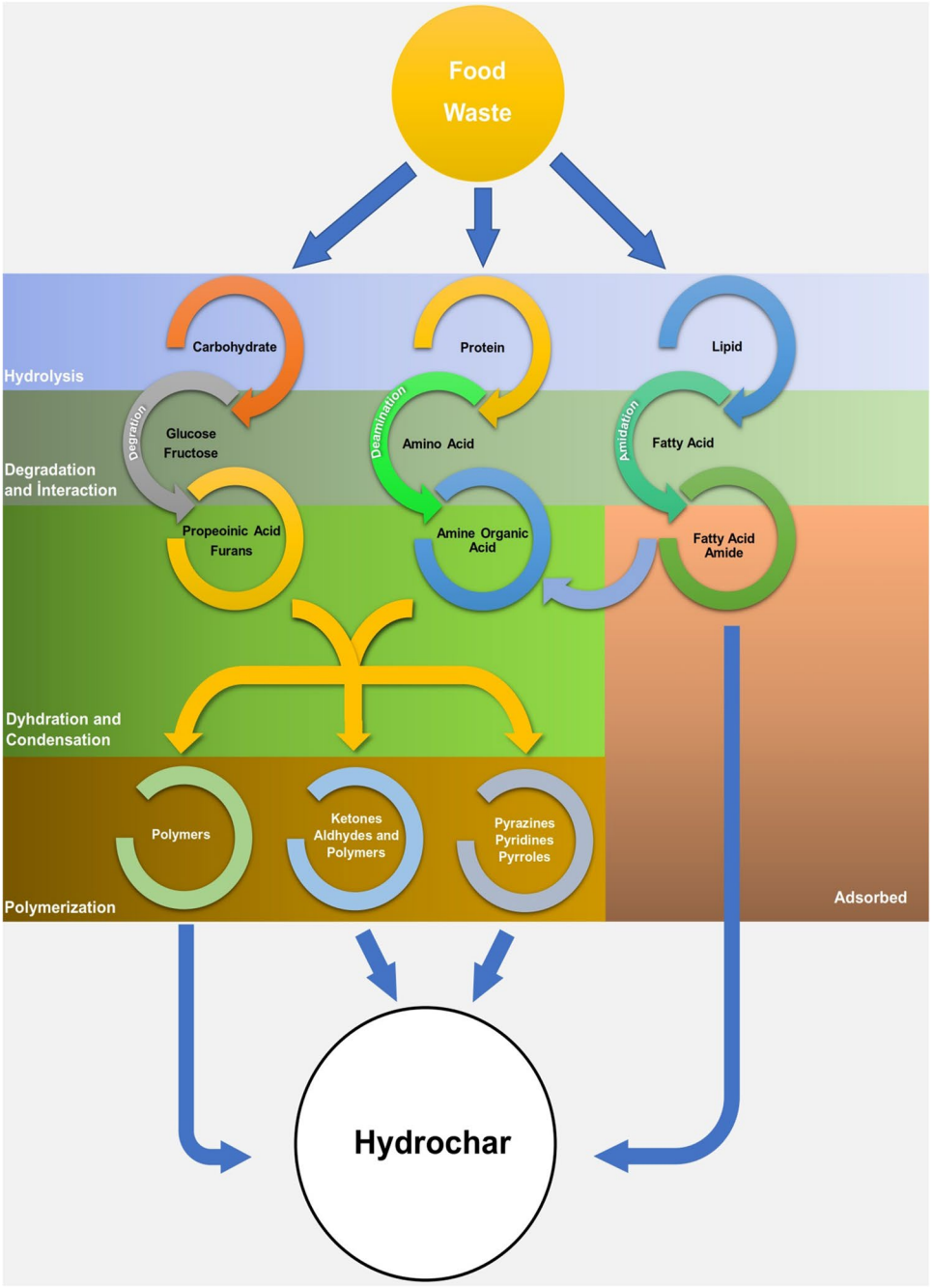

Fig. 6 The mechanism of hydrothermal carbonization process of FW (Yang et al., 2022)

hydrochar-based food waste [1]. The basic reaction mechanism for hydrothermal carbonization of food waste is shown below. The reaction mechanism of food waste leading to the formation of hydrochar, as shown in Fig. 6, was described by Yang et al. [47] discussed.

In the hydrolysis stage, carbohydrates, proteins, and lipids are hydrolyzed into glucose, amino acid, glycerol, and fatty acid, respectively. For example, according to Khan et al. [46], the polysaccharide (including starch and sucrose) component of food waste is converted into its basic units, glucose, and fructose, through the hydrolysis reaction (100–175 °C). In the degradation and interaction section, glucose is broken down into furfural and propenoic acid. Amino acid underwent deamination and decarboxylation to produce organic acid and gas [47]. Additionally, dehydration, deamination, and decarboxylation are used to convert intermediates into furans, heterocyclic, furfural, carbon amine compounds, aldols, benzene-containing derivatives, and condensed ring aromatic hydrocarbons [1]. Lipids gradually decompose into fatty acids and glycerol in a hydrothermal environment. Further hydrolysis of fatty acids to produce hydrocarbon compounds occurs by dehydration and decarboxylation reactions. Finally, these hydrocarbons are polymerized into hydrochar [48].

4 Conclusions

The hydrochar obtained in this study was obtained from SBP by hydrothermal carbonization method under optimum conditions. Reaction parameters were optimized to maximize the %yield and %carbon amount of the hydrochar product. The hydrochar product produced under optimum conditions has higher carbon content than the raw material and therefore has a higher HHV value. High HHV is an advantage in terms of fuel properties. Combustion parameters of SBP and SBP-HC products were determined using thermogravimetric analysis results. According to combustion parameters, the ignition temperature (T_i) of the hydrochar product is also higher compared to the raw material. These results explained that the hydrochar product produced under optimum conditions had better fuel performance compared to the raw material. FT-IR analysis results showed that the SBP-HC product contained oxygen-rich functional groups (C = O-, C-O). SEM results showed that the structure of the SBP-HC product was slightly porous. SEM results showed that the structure of the SBP-HC product was slightly porous. According to FT-IR and SEM analysis results, the hydrochar product produced under optimum conditions can be used in adsorption studies. In addition, the fuel quality of SBP has been improved with the HTC method. Therefore, the SBP-HC product can be considered a biofuel material.

Author contribution This article is a single-author article.

Funding Open access funding provided by the Scientific and Technological Research Council of Türkiye (TÜBİTAK).

Data availability All data generated or analyzed during this study are included in this published article.

Declarations

Ethics approval Not applicable.

Competing interests The author declares no competing interests.

References

1. Le HS, Chen WH, Ahmed SF, Said Z, Rafa N, Le AT, Ağbulut Ü, Veza I, Nguyen XP, Duong XQ, Huang Z, Hoang AT (2022) Hydrothermal carbonization of food waste as sustainable energy conversion path. Bioresour Technol 363:127958
2. Periyavaram SR, Bella K, Uppala L, Reddy PHP (2023) Hydrothermal carbonization of food waste: process parameters optimization and biomethane potential evaluation of process water. J Environ Manage 347:119132
3. Ding Y, Li D, Lv M, Yuan L, Zhang J, Qin S, Wang B, Cui X, Guo C, Zhao P (2023) Influence of process water recirculation on hydrothermal carbonization of rice husk at different temperatures. J Environ Chem Eng 11:109364
4. Pauline AL, Joseph K (2020) Hydrothermal carbonization of organic wastes to carbonaceous solid fuel –a review of mechanisms and process parameters. Fuel 279:118472
5. Nawaz A, Kumar P (2023) Impact of temperature severity on hydrothermal carbonization: fuel properties, kinetic and thermodynamic parameters. Fuel 336:127166
6. Wu S, Wang Q, Fang M, Wu D, Cui D, Pana S, Bai J, Xu F, Wang Z (2023) Hydrothermal carbonization of food waste for sustainable biofuel production: advancements, challenges, and future prospects. Sci Total Environ 897:165327
7. Ma R, Fakudze S, Shang Q, Wei Y, Chen J, Liu C, Han J, Chu Q (2021) Catalytic hydrothermal carbonization of pomelo peel for enhanced combustibility of coal/hydrochar blends and reduced CO_2 emission. Fuel 304:121422
8. Yu Y, Guo Y, Wang G, El-Kassaby YA, Sokhansanj S (2022) Hydrothermal carbonization of waste ginkgo leaf residues for solid biofuel production: hydrochar characterization and its pelletization. Fuel 324:124341
9. McGaughy K, Reza MT (2018) Hydrothermal carbonization of food waste: simplified process simulation model based on experimental results. Biomass Conv Bioref 8:283–292

10. Ronix A, Pezoti O, Souza LS, Souza IPAF, Bedin KC, Souza PSC, Silva TL, Melo SAR, Cazetta AL, Almeida VC (2017) Hydrothermal carbonization of coffee husk: optimization of experimental parameters and adsorption of methylene blue dye. J Environ Chem Eng 5:4841–4849
11. Hossain MA, Ganesan P, Jewaratnam J, Chinna K (2017) Optimization of process parameters for microwave pyrolysis of oil palm fiber (OPF) for hydrogen and biochar production. Energy Convers Manage 133:349–362
12. Wilk M, Sliz M, Gajek M (2021) The effects of hydrothermal carbonization operating parameters on high-value hydrochar derived from beet pulp. Renew Energy 177:216–228
13. Gür E, Semerci TG, Semerci F (2022) Sugar beet pulp derived oxygen-rich porous carbons for supercapacitor applications. J Energy Storage 51:104363
14. Cheng C, Guo Q, Ding L, Raheem A, He Q, Lam SS, Yu G (2022) Upgradation of coconut waste shell to value-added hydrochar via hydrothermal carbonization: parametric optimization using response surface methodology. Appl Energy 327:120136
15. Sharma HB, Sarmah AK, Dubey B (2020) Hydrothermal carbonization of renewable waste biomass for solid biofuel production: a discussion on process mechanism, the influence of process parameters, environmental performance and fuel properties of hydrochar. Renew Sustain Energy Rev 123:109761
16. Ercan B, Alper K, Uçar S, Karagöz S (2023) Comparative studies of hydrochars and biochars produced from lignocellulosic biomass via hydrothermal carbonization, torrefaction and pyrolysis. J Energy Inst 109:101298
17. Zulkornain MF, Shamsuddin AH, Normanbhay S, Saad JM, Zamri MFMA (2022) Optimization of rice husk hydrochar via microwave-assisted hydrothermal carbonization: fuel properties and combustion kinetics. Bioresour Technol Rep 17:100888
18. Saqib NU, Baroutian S, Sarmah AK (2018) Physicochemical, structural and combustion characterization of food waste hydrochar obtained by hydrothermal carbonization. Biores Technol 266:357–363
19. Rajamohan S, Chidambaresh S, Sundarrajan H, Balakrishnan S, Sirohi R, Cao DN, Hoang AT (2023) Investigation of thermodynamic and kinetic parameters of Albizia lebbeck seed pods using thermogravimetric analysis. Biores Technol 384:129333
20. Abnisa F, Daud WMAW, Sahu JN (2011) Optimization and characterization studies on bio-oil production from palm shell by pyrolysis using response surfacemethodology. Biomass Bioenergy 35:3604–3616
21. Sarker TR, Nanda S, Dalai AK (2023) Parametric studies on hydrothermal gasification of biomass pellets using Box-Behnken experimental design to produce fuel gas and hydrochar. J Clean Prod 388:135804
22. Wang Z, Burra KG, Lei T, Gupta AK (2021) Co-pyrolysis of waste plastic and solid biomass for synergistic production of biofuels and chemicals-a review. Prog Energy Combust Sci 84:100899
23. Ighalo JO, Rangabhashiyam S, Dulta K, Umeh CT, Iwuozor KO, Aniagor CO, Eshiemogie SO, Iwuchukwu FU, Igwegbe CA (2022) Recent advances in hydrochar application for the adsorptive removal of wastewater pollutants. Chem Eng Res Des 184:419–456
24. Fang J, Zhan L, Ok YS, Gao B (2018) Minireview of potential applications of hydrochar derived from hydrothermal carbonization of biomass. J Ind Eng Chem 57:15–21
25. Zhang Z, Yang J, Qian J, Zhao Y, Wang T, Zhai Y (2021) Biowaste hydrothermal carbonization for hydrochar valorization: Skeleton structure, conversion pathways and clean biofuel applications. Biores Technol 324:124686
26. Kang K, Nanda S, Sun G, Qiu L, Gu Y, Zhang T, Zhu M, Sun R (2019) Microwave-assisted hydrothermal carbonization of corn stalk for solid biofuel production: optimization of process parameters and characterization of hydrochar. Energy 186:115795
27. Wu S, Wang Q, Cui D, Sun H, Yin H, Xu F, Wang Z (2023) Evaluation of fuel properties and combustion behaviour of hydrochar derived from hydrothermal carbonisation of agricultural wastes. J Energy Inst 108:101209
28. Wu S, Wang Q, Cui D, Wang X, Wu D, Bai J, Xu F, Wang Z, Zhang J (2023) Analysis of fuel properties of hydrochar derived from food waste and biomass: evaluating varied mixing techniques pre/ post-hydrothermal carbonization. J Clean Prod 430:139660
29. Ding Y, Guo C, Qin S, Wang B, Zhao P, Cui X (2022) Effects of process water recirculation on yields and quality of hydrochar from hydrothermal carbonization process of rice husk. J Anal Appl Pyrol 166:105618
30. Li Y, Tsenda N, Lia T, Liu H, Yang R, Gai X, Wang H, Shan S (2019) Microwave assisted hydrothermal preparation of rice straw hydrochars for adsorption of organics and heavy metals. Biores Technol 273:136–143
31. Phan KA, Phihusut D, Tuntiwiwattanapun N (2022) Preparation of rice husk hydrochar as an atrazine adsorbent: optimization, characterization, and adsorption mechanisms. J Environ Chem Eng 10:107575
32. Zhao F, Tang L, Jiang H, Mao Y, Song W, Chen H (2023) Prediction of heavy metals adsorption by hydrochars and identification of critical factors using machine learning algorithms. Biores Technol 383:129223
33. Tran TH, Le AH, Pham TH, Nguyen DT, Chang SW, Chung WJ, Nguyen DD (2020) Adsorption isotherms and kinetic modeling of methylene blue dye onto a carbonaceous hydrochar adsorbent derived from coffee husk waste. Sci Total Environ 725:138325
34. Qin X, Meng W, Cheng S, Xing B, Shi C, Nie Y, Wang Q, Xia H (2023) Efficient removal of heavy metal and antibiotics from wastewater by phosphate-modified hydrochar. Chemosphere 345:140484
35. Lu JJ, Chen WH (2015) Investigation on the ignition and burnout temperatures of bamboo and sugarcane bagasse by thermogravimetric analysis. Appl Energy 160:49–57
36. Soria-Verdugo A, Goos E, García-Hernando N (2015) Effect of the number of TGA curves employed on the biomass pyrolysis kinetics results obtained using the distributed activation energy model. Fuel Process Technol 134:360–371
37. Lang Q, Liu Z, Li Y, Xu J, Li J, Liu B, Sun Q (2022) Combustion characteristics, kinetic and thermodynamic analyses of hydrochars derived from hydrothermal carbonization of cattle manure. J Environ Chem Eng 10:106938
38. Sangare D, Chartier A, Moscosa-Santillan M, Gökalp I, Bostyn S (2022) Kinetic studies of hydrothermal carbonization of avocado stone and analysis of the polycyclic aromatic hydrocarbon contents in the hydrochars produced. Fuel 316:123163
39. Raza M, Abu-Jdayil B, Inayat A (2023) Pyrolytic kinetics and thermodynamic analyses of date seeds at different heating rates using the Coats-Redfern method. Fuel 342:127799
40. Ma J, Luo H, Li Y, Liu Z, Li D, Gai C, Jiao W (2019) Pyrolysis kinetics and thermodynamic parameters of the hydrochars derived from co-hydrothermal carbonization of sawdust and sewage sludge using thermogravimetric analysis. Biores Technol 282:133–141
41. Masoumi S, Dalai AK (2020) Optimized production and characterization of highly porous activated carbon from algal-derived hydrochar. J Clean Prod 263:121427
42. Singh RK, Sarkar A (2023) Pyrolysis of torrefied crop residue: optimization using response surface methodology and benefits of bio-char in co-combustion with coal. Ind Crops Prod 199:116786
43. Mohammed IY, Abakr YA, Yusup S, Kazi FK (2017) Valorization of Napier grass via intermediate pyrolysis: optimization using response surface methodology and pyrolysis products characterization. J Clean Prod 142:1848–1866
44. Fallah S, Alavi N, Tavakoli O, Shahsavani A, Sadani M (2023) Optimization of hydrothermal carbonization of food waste as sustainable energy conversion approach: enhancing the properties of hydrochar by landfill leachate substitution as reaction medium and acetic acid catalyst addition. Energy Convers Manage 297:117647
45. Assis EINC, Gidudu B, Chirwa EMN (2022) Hydrothermal carbonisation of paper sludge: effect of process conditions on hydrochar fuel characteristics and energy recycling efficiency. J Clean Prod 373:133775
46 Khan MA, Hameed BH, Siddiqui MR, Alothman AZ, Alsohaimi HI (2022) Hydrothermal conversion of food waste to

carbonaceous solid fuel—a review of recent developments. Foods 11:4036
47. Yang G, Liu H, Li Y, Zhou Q, Jin M, Xiao H, Yao H (2022) Kinetics of hydrothermal carbonization of kitchen waste based on multi-component reaction mechanism. Fuel 324:124693
48. Wang Q, Wu S, Cui D, Pan S, Xu F, Xu F, Wang Z, Li G (2022) Co-hydrothermal carbonization of corn stover and food waste: characterization of hydrochar, synergistic effects, and combustion characteristic analysis. 10(6):108716